ARTICLE

Impact of Eu^{3+} Ions on Physical and Optical Properties of Li_2O-Na_2O-B_2O_3 Glass

N. A. Razak[a], S. Hashim[a], M. H. A. Mhareb[b*], Y. S. M. Alajerami[c], S. A. Azizan[a], N. Tamchek[d]

a. Department of Physics, Universiti Teknologi Malaysia, Skudai Johor 81310, Malaysia
b. Radiation Protection Directorate, Energy and Minerals Regulatory Commission, Amman 11183, Jordan
c. Department of Medical Radiography, Al-Azhar University, Gaza Strip, Palestine
d. Department of Physics, Faculty of Science, Universiti Putra Malaysia, UPM Serdang 43400, Malaysia

(Dated: Received on November 4, 2015; Accepted on February 26, 2016)

The lithium sodium borate glasses doped with Eu^{3+} ion are prepared using melt quenching technique, their structural and optical properties have been evaluated. The density of prepared glasses exhibits an inverse behavior to the molar volume ranging from 2.26 g/cm^3 to 2.43 g/cm^3 and 26.95 cm^3/mol to 26.20 cm^3/mol, respectively. The absence of sharp peaks in XRD patterns confirms the amorphous nature of the prepared glasses. The absorption spectra yield four transitions centered at 391 nm ($^7F_0 \rightarrow {}^5L_6$), 463 nm ($^7F_0 \rightarrow {}^5D_2$), 531 nm ($^7F_0 \rightarrow {}^5D_1$), and 582 nm ($^7F_0 \rightarrow {}^5D_0$). The most intense red luminescence is observed at 612 nm corresponding to $^5D_0 \rightarrow {}^7F_2$ transition under 390 nm laser excitations.

Key words: Absorption, Photoluminescence, Borate glass, Europium oxide

I. INTRODUCTION

The prominence function in various photonic devices has brought the area of photonics into close scrutiny and been put into much attention in the preparation and optimization of novel optical materials, thus, numerous researches are being carried out by choosing appropriate new hosts doped with rare earth (RE) ions. The optical properties of RE ions with their local structure and the interaction with the ligands has a direct governing effect on the performance of these devices, hence a close relationship between these two aspects is of prime importance in the effective development of such devices. Based on this factor, borate-based glasses are one of the best candidates which shows a clear relationship between the glass structure and the optical properties of RE ions. The inclination towards borate glasses is due to their properties of high transparency, low melting point, high thermal stability and good rare earth ion solubility [1]. Another interesting characteristic of the borate glasses is the appearance of variations in its structural properties when alkaline or alkaline-earth cations are introduced. The structure of the borate glasses is not simply a random distribution of BO_3 triangles and BO_4 tetrahedra, rather, a gathering of these units forming a well-defined and stable borate groups such as diborate, triborate, tetraborate, *etc.* that constitute the random three-dimensional network [2].

Despite the superior advantages which enable them as preferred glass formers, the borate alone is easily crystallized and possesses hygroscopic nature which often limits its practical uses. However, these drawbacks have been improvised by incorporating suitable modifiers into the glass network. Incorporation of modifiers enhances the stability and reduces the hygroscopic properties of the glass. Lithium oxide is widely used as modifiers to improve the borate stability. The introduction of lithium ions in the glass mixture leads to the formation of ionic bonds with bridging (BO) and non-bridging oxygen (NBO) atoms [3]. Sodium oxide is also used as a modifier in borate networks. Following the electronic configuration of [Ne]3s^1, the free electron in the outer L-shell of sodium with isoelectric sequence makes it extremely stable, particularly after the loss of extra electron on the 3s level [4].

The introduction of lanthanide (Ln) ions into the glass network is very crucial in the development of optical devices such as solid state lasers, optical detectors, waveguide lasers, optical fiber amplifiers, and field emission displays [5]. The research on Ln-doped glasses is not only limited to infrared optical devices but also in visible optical devices [6]. Amongst Ln^{3+} ions, Eu^{3+} ion is one of the best candidates for the use in photonic application as red emitting phosphors for field-emission technology due to the narrow and monochromatic nature of the $^5D_0 \rightarrow {}^7F_2$ transition at around 610 nm [7]. Persistent spectral hole burning can also be performed in the $^7F_0 \rightarrow {}^5D_0$ transition at room temperature which has potential to be used in high-density optical storage [8]. These optical properties of

*Author to whom correspondence should be addressed. E-mail: mmhareb@hotmail.com

ion are highlysensitive to the surrounding environment. Hence, Eu^{3+} ion is a well-known spectroscopic probe used to estimate the local environment around RE ions in various crystals and glass matrices from its f-f transition spectra. This is majorly attributed to its relatively simple energy level structure with non-degenerate ground $^7F_0$ and emitting $^5D_0$ states [2]. Furthermore, Eu_2O_3-doped phosphors also exhibit higher luminescence efficiency compared with other luminescence materials [9, 10], and therefore Eu^{3+} ion is commonly used in the field emission technology and LEDs [11].

In the present work, we investigate the Eu^{3+} ion concentration dependent physical and the optical properties of lithium sodium borate (LNB) glasses. Melt annealed synthesized glasses are characterized via XRD, FTIR, UV-Vis and PL measurements. Results are analyzed and compared with other reports. The impact of Eu^{3+} ion on the spectral features is demonstrated.

II. EXPERIMENTS

Glasses of $10Na_2O{:}20Li_2O{:}(70-x)B_2O_3{:}xEu_2O_3$ with $0.3 \leq x \leq 1$ are prepared using conventional melt quenching technique. Analytical grade high purity (Aldrich company) powders of Li_2O (99.9%), Na_2O (99.9%), B_2O_3 (99%), and Eu_2O_3 (99.9%) are chosen as raw materials. Boron oxide is the glass former while lithium and sodium oxides are the glass modifiers. Glasses are prepared by mixing a synchronized amount of lithium oxide (Li_2O), sodium oxide (Na_2O) and boron oxide (B_2O_3), followed by the addition of europium oxide (Eu_2O_3) as an activator. The constituents are thoroughly mixed for 30 min to obtain a homogenous mixture before placing the alumina crucible (containing the mixture) inside the electronic furnace at 1100 °C for 1 h. The molten mixture is frequently stirred to achieve complete homogeneity before it is poured onto a steel plate and annealed at 400 °C for 3 h to remove the remaining stress. Upon completing the annealing process, the furnace is switched off and gradually cooled down to room temperature using an average cooling rate of 10 °C/min. Prepared glasses are stored in vacuum desiccators to prevent attacking from moisture and other contaminations. The compositions of the current glasses with their codes are listed in Table I. Samples with 0.3mol%, 0.5mol%, 0.7mol%, 1.0mol% Eu_2O_3 are coded as LNB0.3, LNB0.5, LNB0.7, LNB1.0, respectively.

The amorphous nature of the glasses are examined via a Rigaku AX-2500 Advance X-ray diffractometer which uses Cu-Kα radiations (λ=1.54 Å) at 40 kV and 30 mA with 2θ ranges from 10° to 80°. Fourier transform infrared (FTIR) transmission measurements in the range of 500−2200 cm^{-1} are carried out by a Perkin Elmer FTIR 1660 spectrometer using KBr pellets. The room temperature absorption spectra are recorded in the range of 370−700 nm by using Shimadzu UV-3101PC scanning spectrophotometer (Kyoto, Japan). The emission measurement is performed by Perkin Elmer LS-55 photoluminescence (PL) spectrometer (UK) where a xenon discharge lamp in the wavelength range of 560−720 nm is used as excitation source.

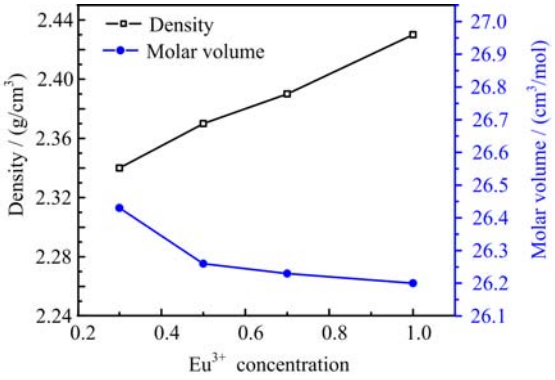

FIG. 1 Variation density and refractive index of LNB glasses for different concentrations of Eu^{3+} ion.

TABLE I Composition of prepared glass samples.

Sample	Composition/mol%			
	Li_2O	B_2O_3	Na_2O	Eu_2O_3
LNB0.3	20	69.7	10	0.3
LNB0.5	20	69.5	10	0.5
LNB0.7	20	69.3	10	0.7
LNB1.0	20	69.0	10	1.0

III. RESULTS AND DISCUSSION

A. Physical properties

The calculated physical parameters for all samples are listed in Table II. The related formulas of physical parameters are described somewhere else [12]. The gradual increase of Eu_2O_3 leads to the enhancement in density and decreasing in molar volume as shown in Fig.1. The increase in density from 2.26 g/cm^3 to 2.43 g/cm^3 is majorly attributed to the enhancement in the molecular mass of the glass host [13]. Meanwhile, the decrease in molar volume from 26.95 cm^3/mol to 26.20 cm^3/mol shows the increase in glass compactness. The polaron radius and the inter-nuclear distance exhibit an inverse behavior to that of density with increasing concentration of europium ions. This increase in packing is ascribed to the crowding of glass network by the europium interstices that reduce the average distance between rare earths and oxygen [14]. The increase in refractive index from 2.309 to 2.363 with the increase of Eu^{3+} ion contents is mainly due to the activation of more ionic dipoles when being exposed to an electric field [13]. The enhancement in the number of

DOI:10.1063/1674-0068/29/cjcp1511226

TABLE II Eu^{3+} ion concentration dependent physical properties of prepared glasses.

	ρ/(g/cm^3)	V/(cm^3/mol)	C/(10^{20} ion/cm^3)	r_p/Å	r_i/Å	$d_{b\text{-}b}$/Å	n	R_m	$\alpha_e\times10^{-24}$
LNB0.3	2.34	26.43	67.33	3.39	5.30	4.169	2.309	18.08	7.17
LNB0.5	2.37	26.26	113.97	2.84	4.44	4.151	2.316	18.01	7.14
LNB0.7	2.39	26.23	161.22	2.53	3.96	4.139	2.343	18.14	7.19
LNB1.0	2.43	26.20	233.65	2.24	3.50	4.125	2.363	18.24	7.23

Note: the parameters ρ, V, C, r_p, r_i, $d_{b\text{-}b}$, n, R_m, and α_e represent density, molar volume, ion concentration, polaron radius, inter nuclear distance, boron-boron separation, refractive index, molar refractivity, and polarizability, respectivly.

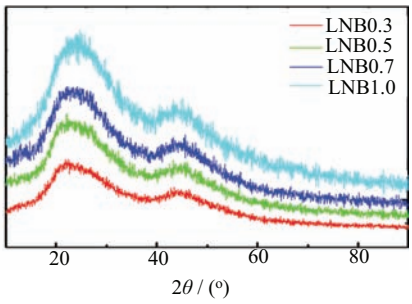

FIG. 2 XRD patterns of LNB glasses with different concentrations of Eu^{3+} ion.

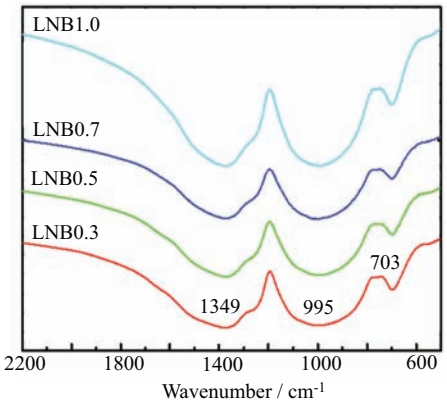

FIG. 3 FTIR spectra of LNB glasses with different concentrations of Eu^{3+} ion.

non-bridging oxygen and large polarizability also leads to an increase in refractive index [15]. The decrease in boron-boron distance originates from the stretching force of the bonds in the glass network [15].

B. XRD and FTIR spectra

The XRD patterns of LNB glasses are shown in Fig.2. The presence of a broad hump confirms the amorphous nature of prepared glasses.

The IR spectra show prominent bands which are attributed to the active vibration of borate network. These bands can be classified into three infrared groups which are similar to those reports in Refs.[16, 17]. The band around 1200−1600 cm^{-1} is identified as the asymmetric stretching relaxation of the bond between borate trigonal BO_3 and oxygen units. The band that appears in the region of 800−1200 cm^{-1} is assigned to the stretching vibration of BO_4 units where BO_3 units (sp^2) are converted into tetrahedral BO_4 units (sp^3). The band at 700 cm^{-1} is allocated to the bending vibration of B−O linkages in the borate network. Figure 3 illustrates the FTIR spectra of all the glasses. The bending of B−O linkages in borate network is assigned at a wavelength of 703 cm^{-1}. Meanwhile, the band evidenced at the wavelength of 995 cm^{-1} is contributed by the phenomena where BO_3 units (sp^2) are converted into tetrahedral BO_4 units (sp^3). Finally, the band at 1349 cm^{-1} originates from the asymmetric stretching relaxation of the bond between borate trigonal BO_3 and oxygen unit. The IR spectra for all concentrations are almost consistent. The addition of lithium and sodium oxide into the glass network is found to result the conversion of sp^2 planar (BO_3 unit) into a more stable sp^3 planar (BO_4 unit) by creating a new non-bridging oxygen bond [16]. The bands at 703, 995, 1349 cm^{-1} are assigned as bending vibrations O−B−Eu, B−O stretching of tetrahedral BO_4 unit, and B−O stretching of trigonal BO_3 unit.

C. Absorption and emission spectra

The optical absorption spectra of LNB glasses doped with Eu^{3+} ion in the range of 350−700 nm is shown in Fig.4. The absorption spectra of the glasses yield four transitions centered at 388 nm ($^7F_0\rightarrow{}^5L_6$), 463 nm ($^7F_0\rightarrow{}^5D_2$), 531 nm ($^7F_0\rightarrow{}^5D_1$) and 582 nm ($^7F_0\rightarrow{}^5D_0$). The bands' assignments of the absorption spectra are in agreement with other studies [18, 19]. These absorption bands are attributed to the characteristics f→f optical transitions of Eu^{3+} ion between the ground and excited levels [18]. It is observed that the $^7F_0\rightarrow{}^5L_6$ absorption band is found to be more intense than all other transitions, although it is forbidden by ΔS and ΔL selection rules, it is allowed by ΔJ selection rule [18]. The $^7F_0\rightarrow{}^5D_0$ transition is forbidden by the two former selection rules, hence it exhibits a rela-

DOI:10.1063/1674-0068/29/cjcp1511226

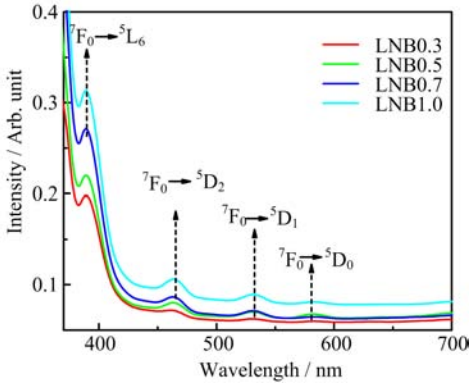

FIG. 4 UV-Vis-NIR absorption spectra of LNB glasses with different concentrations of Eu^{3+} ion.

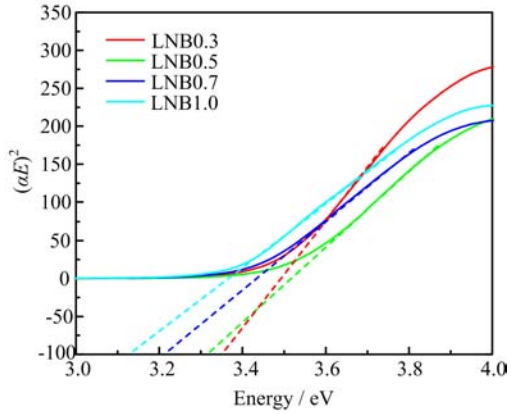

FIG. 5 Direct optical band gap energy of LNB glasses with different concentrations of Eu^{3+} ion.

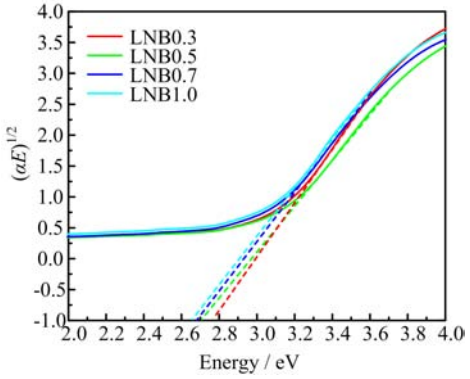

FIG. 6 Indirect optical band gap energy of LNB glasses with different concentrations of Eu^{3+} ion.

TABLE III Eu^{3+} ion concentration dependent direct optical band gap, indirect optical band gap and Urbach energy for all samples.

Glasses	Energy/eV		
	Direct	Indirect	Urbach
LNB0.3	3.35	2.78	0.372
LNB0.5	3.32	2.70	0.385
LNB0.7	3.21	2.68	0.391
LNB1.0	3.13	2.65	0.394

tively weak intensity [6]. The magnetic dipole allowed $^7F_0 \rightarrow {}^5D_1$ transition is relatively weaker than the electric dipole allowed $^7F_0 \rightarrow {}^5D_2$ transition for LNB glasses doped with Eu^{3+} ion. The $^7F_0 \rightarrow {}^5D_3$ transition has not been observed, since it is forbidden by the selection rule (ΔJ=3) [2].

The study of the fundamental absorption edge in the UV-region is useful to investigate the optical transitions and the electronic band structure in crystalline and non-crystalline materials. There are direct and indirect optical transitions that can occur at the fundamental absorption edge of crystalline and non-crystalline materials. In both cases, electromagnetic waves interact with electrons in the valence band, which are raised across the fundamental gap to the conduction band [20]. The details of direct and indirect transition calculation used in this work can be referred in Ref.[21]. Figures 5 and 6 display the Tauc plot for estimating the direct and indirect band gap energies. The europium concentration dependent optical band gap energies for both direct and indirect transitions are summarized in Table III. The direct and indirect optical band gap energies are found to decrease in the range of 3.35 eV to 3.13 eV and 2.78 eV to 2.65 eV, respectively. The decrease in gap energy with the successive addition of Eu^{3+} is attributed to the structural changes in the prepared glasses. The increase in Eu^{3+} contents may enhance the degree of localization by creating defect in the charge distribution and drive the energy levels of the closet oxygen ions near to the top of the valence band and thereby raise donor centers in the glass matrix [15]. The increase in donor centers leads to a decrease in energy band gap.

For varying Eu_2O_3 contents, the Urbach energies of LNB glasses are shown in Fig.7. Calculated from the inverse slope, the Urbach energies of LNB glasses are found to lie between 0.372 and 0.394 eV, the relation between direct optical band gap energy and Urbach energy is shown in Fig.8. It shows that as the direct optical band gap increases, the Urbach energy decreases. The observed increase in the Urbach energy with the increase of Eu^{3+} concentration is mainly due to the formation of bonding defects and non-bridging oxygen. These values are well within the range of 0.046−0.66 eV for amorphous semiconductors [15].

Figure 9 shows the Eu^{3+} ion concentration dependent room temperature emission spectra of all samples under 390 nm laser excitations. The luminescence spectra consist of five characteristic emission bands at 576, 587, 612, 652, and 699 nm. Sample with 0.5mol% of Eu_2O_3 content exhibits maximum peak intensity and intensity quenching is observed beyond this concentration. The increasing of Eu_2O_3 content leads the population of Eu^{3+} ions at the $^5D_0$ level to increase, hence the PL intensity increases due to the improved sponta-

DOI:10.1063/1674-0068/29/cjcp1511226

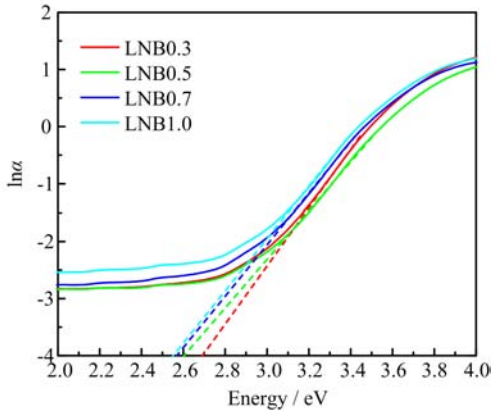

FIG. 7 Urbach energy of LNB glasses for different concentrations of Eu^{3+} ion.

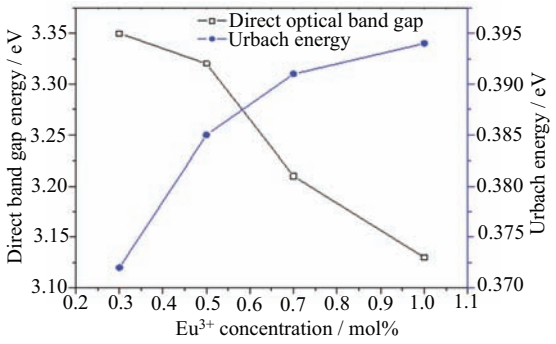

FIG. 8 Variation direct optical band gap energy and Urbach energy of LNB glasses for different concentrations of Eu^{3+} ion.

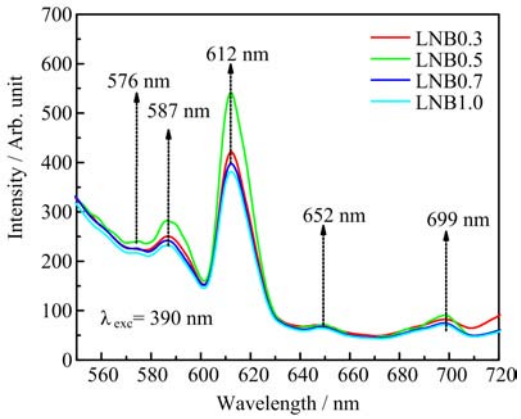

FIG. 9 Emission spectra of LNB glasses for different concentrations of Eu^{3+} ion.

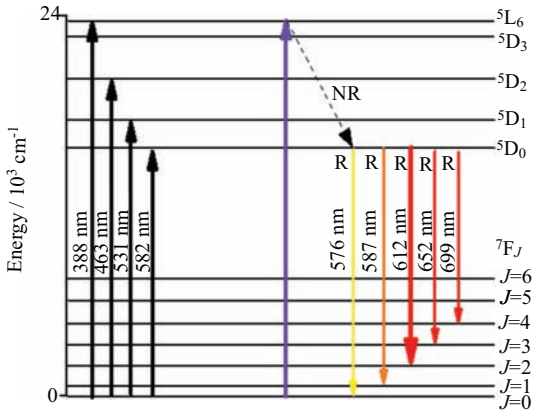

FIG. 10 The energy level diagram of Eu^{3+} ion showing possible transition pathways and other processes under 390 nm excitations.

neous radiation transitions. However, the gradual enhancement in the concentration causes the quenching effect to induce the emission to some extent becomes weaker. The quenching phenomenon explains that, at a certain limiting concentration, RE ions are spaced closely enough allowing the energy exchange between neighboring ions to occur until the excitation ion comes to a less excited state [22]. The transition from this less excited state to the ground state is non-radiative (NR), causing the luminescence to completely quench. Consequently, 0.5mol% is an optimum Eu_2O_3 concentration to enhance the red fluorescence.

The excitation and emission mechanisms are presented in Fig.10. The absence of emissions starting from the excited levels of ^5D_J (J=3,2,1) is due to the high energy phonons found in the glasses, for example, when the Eu^{3+} ions are excited to any level above the $^5D_0$, there is a fast NR multiphonon relaxation to this level. The emission from $^5D_{3,2,1}\rightarrow{}^7F_J$ are several orders smaller than that of $^5D_0\rightarrow{}^7F_J$, which causes emissions from these three excited states to be suppressed, therefore $\Sigma{}^5D_0\rightarrow{}^7F_J$ emission intensity represents the total intensity of the Eu^{3+} glass studied [23−27]. From $^5D_0$ level the Eu^{3+} ions decay radiatively (R), since the large energy difference of the $^7F_6$ level prevents the possibility of multiphonon relaxation. Due to high NR relaxation from excited states of energy higher than $^5D_0$ state, the intense emission bands are caused by the $^5D_0\rightarrow{}^7F_J$ (J=0, 1, 2, 3, and 4) transitions. The five emission transitions namely $^5D_0\rightarrow{}^7F_0$ (576 nm), $^5D_0\rightarrow{}^7F_1$ (587 nm), $^5D_0\rightarrow{}^7F_2$ (612 nm), $^5D_0\rightarrow{}^7F_3$ (652 nm) and $^5D_0\rightarrow{}^7F_4$ (699 nm). The emission transitions are comparable with those obtained for other reported glasses [23−27]. The most intense and long-lived luminescence at $^5D_0\rightarrow{}^7F_2$ (612 nm) shows a strong red emission and demonstrates its potential application as a red-emitting glass material. Among the $^5D_0\rightarrow{}^7F_J$ transitions, the selection rules make the $^5D_0\rightarrow{}^7F_1$ and $^5D_0\rightarrow{}^7F_2$ transitions are of the particular interest. The $^5D_0\rightarrow{}^7F_2$ transition is considered as a hypersensitive transition following the selection rules of ΔJ=2. The $^5D_0\rightarrow{}^7F_1$ transition with ΔJ=1 is found to be an allowed magnetic dipoles (MD) and its intensity is generally independent of the crystal field strength around the Eu^{3+} ion. This transition could be used for the estimation of transition probabilities of various excited levels. The transitions of $^5D_0\rightarrow{}^7F_J$ with J=5 and J=6 are not observed due to

DOI:10.1063/1674-0068/29/cjcp1511226

significantly weak transition probabilities. The analysis on the emission transitions are based on the reports in Refs.[6, 11].

IV. CONCLUSION

Modifications in physical and optical properties of LNB glasses at various doping levels of Eu^{3+} ion are determined. Conventional melt quenching method is used to prepare glasses. The density is found to increase, meanwhile the molar volume is found to decrease with the gradual addition of Eu^{3+} ion contents. The increase in density is due to the increasing of molecular mass of the glass host. The stretching vibration of BO_4 units accompanied by the conversion of BO_3 (sp^2) into tetrahedral BO_4 units (sp^3) is observed. The decrease in optical band gap energies with the increase of Eu^{3+} ions concentration is ascribed to structural alterations and increase in donor centers in the glass matrix. The UV-Vis spectra reveal four absorption bands and the PL spectra exhibit an intense red luminescence at 612 nm corresponding to $^5D_0 \rightarrow {}^7F_2$ transition. The superior structural and optical features of these new glass compositions offer them as suitable candidate for red laser source applications.

V. ACKNOWLEDGMENTS

This work was supported by the Research University Grant Scheme from UTM, Vote number (10H60) and UTM Zamalah Scholarship.

[1] V. Venkatramu, P. Babu, and C. K. Jayasankar, Spectrochim. Acta Part A **63**, 276 (2006).
[2] V. Lavin, P. Babu, C. K. Jayasankar, I. R. Martin, and V. D. Rodriguez, J. Chem. Phys. **115**, 10935 (2001).
[3] M. H. A. Mhareb, S. Hashim, A. S. Sharbirin, Y. S. M. Alajerami, R. S. E. S. Dawaud, and N. Tamchek, Opt. Spectrosc. **117**, 552 (2014).
[4] Y. Alajerami, S. Hashim, W. M. S. Wan Hassan, A. T. Ramli, and M. I. Saripan, Opt. Spectrosc. **114**, 537 (2013).
[5] L. Zur, J. Janek, M. Soltys, J. Pisarska, and W. A. Pisarski, Phys. Scr. **T157**, 014035 (2013).
[6] C. R. Kesavulu, K. K. Kumar, N. Vijaya, K. Lim, and C. K. Jayasankar, J. Chem. Phys. **141**, 903 (2013).
[7] K. Linganna and C. K. Jaysankar, Spectrochim. Acta Part A **97**, 788 (2012).
[8] D. E. Day, J. Non-Cryst. Solids **21**, 343 (1976).
[9] Q. Y. Zhang, K. Pita, W. Ye, and W. X. Que, Chem. Phys. Lett. **351**, 163 (2002).
[10] J. K. Park, M. A. Lim, C. H. Kim, H. D. Park, J. T. Park, and S. Y. Choi, Appl. Phys. Lett. **82**, 683 (2003).
[11] B. D. P. Raju and C. Madhukar Reddy, Opt. Mater. **34**, 1251 (2012).
[12] S. A. Azizan, S. Hashim, N. A. Razak, M. H. A. Mhareb, Y. S. M. Alajerami, and N. Tamchek, J. Mol. Struct. **1076**, 20 (2014).
[13] S. A. Reduan, S. Hashim, Z. Ibrahim, Y. S. M. Alajerami, M. H. A. Mhareb, M. Maqableh, R. S. E. S. Dawaud, and N. Tamchek, J. Mol. Struc. **1076**, 6 (2014).
[14] R. S. Gedam and D. D. Ramteke, J. Rare Earths **30**, 785 (2012).
[15] M. H. A. Mhareb, S. Hashim, S. K. Ghoshal, Y. S. M. Alajerami, M. A. Saleh, R. S. Dawaud, N. A. B. Razak, and S. A. B. Azizan, Opt. Mater. **37**, 391 (2012).
[16] R. B. Rao and N. Veeraiah, Physica B **348**, 256 (2004).
[17] I. A. Rayappan and K. Marimuthu, J. Phys. Chem. Solids **74**, 1570 (2013).
[18] P. Babu and C. K. Jayasankar, Physica B **279**, 262 (2000).
[19] K. Selvaraju, K. Marimuthu, T. K. Seshagiri, and S. V. Godbole, Mater. Chem. Phys. **131**, 204 (2011).
[20] R. P. S. Chakradhar, K. P. Ramesh, J. L. Rao, and J. Ramakrishna, J. Phys. Chem. Solids **64**, 641 (2003).
[21] E. A. Davis and N. F. Mott, Phill. Mag. **22**, 903 (1970).
[22] I. Jlassi, H. Elhouichet, M. Ferid, R. Chtourou, and M. Oueslati, Opt. Mater. **32**, 743 (2010).
[23] N. Wada and K. Kojima, J. Lumin. **126**, 53 (2007).
[24] M. M. A. Maqableh, S. Hashim, Y. S. M. Alajerami, M. H. A. Mhareb, R. S. Dawwud, and A. Saidu, Opt. Spectrosc. **117**, 67 (2014).
[25] C. H. Kam and S. Buddhudu, Physica B **344**, 182 (2004).
[26] S. Surendra Babu, P. Babu, C. K. Jayasankar, W. Sievers, T. Troster, and G. Wortmann, J. Lumin. **126**, 109 (2007).
[27] M. Rodriguez, A. Cardenas, E. Castiglioni, J. Castiglioni, J. F. Carvalho, and L. Fornaro, J. Non-Cryst. Solids **401**, 181 (2014).

DOI:10.1063/1674-0068/29/cjcp1511226